Available online at www.sciencedirect.com

ScienceDirect

Procedia Engineering 136 (2016) 88 – 94

Procedia Engineering

www.elsevier.com/locate/procedia

The 20th International Conference: Machine Modeling and Simulations, MMS 2015

Numerical prediction of fusion zone and heat affected zone in hybrid Yb:YAG laser + GMAW welding process with experimental verification

Marcin Kubiak[a,*], Wiesława Piekarska[a], Zbigniew Saternus[a], Tomasz Domański[a]

[a] *Institute of Mechanics and Machine Design Foundations, Częstochowa University of Technology, Dabrowskiego 73, 42-200 Częstochowa, Poland*

Abstract

This work concerns mathematical and numerical modelling of temperature field during hybrid welding process using Yb:YAG laser and electric arc in GMAW method. Numerical analysis is performed taking into account the motion of liquid steel in the fusion zone. Yb:YAG laser power distribution is determined on the basis of experimental research made on TruDisk 12002 laser. Geostatistical Kriging method is used in the interpolation of Yb:YAG laser power intensity distribution. Temperature field and melted material velocity field in the fusion zone of hybrid welded sheets made of S355 steel are obtained on the basis of numerical solution of continuum mechanics equations in Chorin's projection method and finite volume method. Experimental research of laser beam profile is performed in order to verify the correctness of developed heat source model. Fusion zone and heat affected zone geometry is predicted on the basis of calculated temperature field in the cross section of hybrid welded joint.

Peer-review under responsibility of the organizing committee of MMS 2015

Keywords: hybrid welding; Yb:YAG laser; heat source; thermal phenomana; phase transformations; heat affected zone

* Corresponding author. Tel.: +48 34 325 06 51; fax: +48 34 325 06 47.
E-mail address: kubiak@imipkm.pcz.pl

Peer-review under responsibility of the organizing committee of MMS 2015
doi:10.1016/j.proeng.2016.01.179

1. Introduction

Because of technological advantages of laser materials processing, this technology successfully displaces conventional production techniques in many applications, including welding. However, technological difficulties as well as the need for a precise fit-up of welded parts (especially when combining elements of large thickness) in some cases limit its application [1]. Therefore, alternative methods are still looked for.

The combination of laser beam welding with popular and well-known electric arc welding [2] cooperating in a single process is under particular attention in recent years. Especially when using modern Yb:YAG laser [3] in this hybrid welding process.

The knowledge about thermal phenomena occurring in welding process is crucial in the prediction of the quality and durability of welded construction. Therefore, research is focused on mathematical modeling and numerical analysis [4–8]. Computer simulations allow for a prediction of chosen process parameters that can be used in industrial practice. However, modeling of thermal phenomena in welding process using laser beam heat source requires a new approach to the theory and numerical solution techniques, because heat distribution proceeds in different conditions in comparison to classic welding techniques. Moreover, the laser beam intensity distribution models assumed in numerical analysis significantly differ from real Yb:YAG laser profile, obtained through experimental research [9, 10]. Therefore, more sophisticated laser beam heat source models are necessary to describe the real process conditions with a proper accuracy.

This work concerns mathematical and numerical modelling of thermal phenomena occurring in laser-arc hybrid butt-welding of thin elements made of S355 steel. The motion of liquid steel in the fusion zone is taken into considerations in the analysis as well as the latent heat generated during materials' state changes. Modelled thermal phenomena as a three-dimensional case are presented in a scheme of the considered system (Fig. 1).

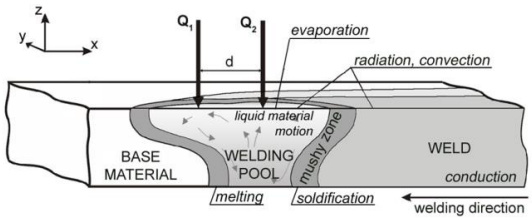

Fig. 1. Schematic sketch of laser-arc hybrid welding simulation.

2. Mathematical modelling

The temperature field and liquid material velocity field are determined on the basis of the solution of mass, momentum and energy conservation equations, described as follows:

$$\frac{\partial \rho}{\partial t} + \frac{\partial}{\partial x_i}\left(\rho v_i\right) = 0 \tag{1}$$

$$\frac{\partial\left(\rho v_i\right)}{\partial t} + \frac{\partial}{\partial x_j}\left(\rho v_i v_j\right) = -\frac{\partial p}{\partial x_i} + \frac{\partial}{\partial x_j}\left(\mu \frac{\partial v_i}{\partial x_j}\right) + \mathbf{g}\beta_T\left(T - T_{ref}\right) - \frac{\mu}{\rho K} v_i \tag{2}$$

$$\frac{\partial}{\partial x_i}\left(\lambda \frac{\partial T}{\partial x_i}\right) = C_{ef}\left(\frac{\partial T}{\partial t} + v_i \frac{\partial T}{\partial x_i}\right) - \widetilde{Q} \tag{3}$$

where ρ is density (kg.m^{-3}), g is gravity acceleration β_T is thermal expansion coefficient (K^{-1}), μ is dynamic viscosity (kg.ms^{-1}), T_s is the solidus temperature K is porous medium permeability, $\lambda = \lambda(T)$ is conductive coefficient (W.m^{-1}.K^{-1}), $C_{ef} = C_{ef}(T)$ is an effective heat capacity $\widetilde{Q}$ is laser beam heat source power over the area (W.m^{-3}), $\mathbf{v} = \mathbf{v}(x_\alpha,t) = (u,v,w)$ is a velocity vector, $T = T(x_\alpha,t)$ is a temperature and subscripts i, j stand for material point coordinates.

Governing equations are completed by the initial and boundary condition. Eq. (2) is completed by the initial condition $t = 0 : \mathbf{v} = 0$ and Dirichlet type boundary condition $\mathbf{v}\big|_{T=T_S} = 0$ at the boundaries determined by the solidus temperature (melted zone boundary). Marangoni effect is considered [6] at the top surface of welded plate. Energy conservation equation (3) is completed by the initial condition $t = 0 : T = T_0$ and boundary conditions of Neumann and Newton type taking into account the heat loss due to convection and radiation [5, 8].

Solidification process can be analyzed in micro [11, 12] or macro scale [4, 6, 8]. Macro model with effective heat capacity is used in this study. Effective capacity is defined assuming linear approximation of solid fraction in the mushy zone and liquid fraction in liquid-gas region:

$$C_{ef}(T) = \begin{cases} \rho_S c_S & \text{for} \quad T < T_S \\ \rho_{SL} c_{SL} + \rho_S \dfrac{H_L}{T_L - T_S} & \text{for} \quad T \in [T_S ; T_L] \\ \rho_L c_L & \text{for} \quad T \in [T_L ; T_b] \\ \rho_L c_L + \dfrac{\rho_L H_b}{T_{\max} - T_b} & \text{for} \quad T \in [T_b ; T_{\max}] \end{cases} \tag{4}$$

where subscripts S and L denote solid and liquid state, c is a specific heat (c_S = 650 J.kg^{-1}.K^{-1}, c_L=840 J.kg^{-1}.K^{-1}), ρ is density (ρ_S = 7800 kg.m^{-3}, ρ_L = 6800 kg.m^{-3}), T_S = 1750 K and T_L = 1800 K are solidus and liquidus temperatures respectively, $H_L = 270 \cdot 10^3$ J.kg^{-1} is a latent heat of fusion, T_b = 3010 K is the boiling point of steel, T_{max} is the maximum temperature of thermal cycle, $H_b = 76 \cdot 10^5$ J.kg^{-1} is a latent heat of evaporation. The product of density and specific heat in the mushy zone depends linearly on solid fraction $\rho_{SL} c_{SL} = \rho_S c_S f_S + \rho_L c_L (1 - f_S)$, where $f_S \in [0;1]$ is the solid fraction.

A very important step during the numerical analysis of welding processes is the proper selection of the heat source power distribution, primarily responsible for the melted pool and heat affected zone shape. Defined in Eq. (5) 'double ellipsoidal' heat source [13] bellow the welding arc (Q_1) is used in this study (Fig. 2). This heat source model can be used to simulate various arc parameters and has very good features of power density distribution control in the weld and HAZ:

$$Q_1 = \begin{cases} q_1(x,y,z) = \dfrac{6\sqrt{3} f_1 Q_A}{abc_1 \pi \sqrt{\pi}} \times \exp(-3\dfrac{x^2}{c_1^2}) \times \exp(-3\dfrac{y^2}{a^2}) \times \exp(-3\dfrac{z^2}{b^2}) & \text{for } x < x_o \\ q_2(x,y,z) = \dfrac{6\sqrt{3} f_2 Q_A}{abc_2 \pi \sqrt{\pi}} \times \exp(-3\dfrac{x^2}{c_2^2}) \times \exp(-3\dfrac{y^2}{a^2}) \times \exp(-3\dfrac{z^2}{b^2}) & \text{for } x \geq x_o \end{cases} \tag{5}$$

where a, b, c_1 and c_2 are set of axes that define front ellipsoid and rear ellipsoid, f_1 and f_2 ($f_1 + f_2 = 2$) represent distribution of the source energy at the front and the rear section of the source and $Q_A = \eta_A IU$ is the arc heat source power, where I is current intensity, U is voltage and η_A is efficiency of the electric arc.

Yb:YAG laser heat source (Q_2) power distribution (Fig. 3) is determined using interpolation algorithms. Among various interpolation algorithms ordinary Kriging method [10, 14] is used in this study in the form of point Kriging allowing a precise description of Yb:YAG laser power intensity distribution, taking into account the real laser power distribution obtained in experimental research made on laser welding station equipped with TruDisk 12002 laser.

The laser beam heat source power distribution is calculated assuming the linear decrease of energy intensity with material penetration, according to the following formula:

$$Q_2(x,y,z) = \eta_L Q_L \tilde{f}(x,y)\left(1-\frac{z}{s}\right) \tag{6}$$

where η_A is the absorption coefficient, $Q_L = \alpha P/\pi\omega_0^2 s$ is the laser power per unit area (W.m^{-2}), P is pumped power (W), ω_0 is a radius of the beam (m), s is the heat source penetration depth (m), α is a heat source coefficient (for the cone like shape of the volume of a heat source the distribution $\alpha = 3$), function $\tilde{f}$ is Kriging interpolation defined as a linear combination of observations in basic points (the real power distribution), estimated as a function of the weighted average.

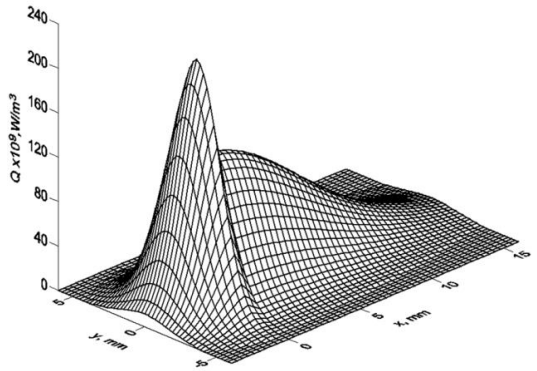

Fig. 2. Exemplary Goldak's heat source distribution at the top surface (z = 0) of welded sheets.

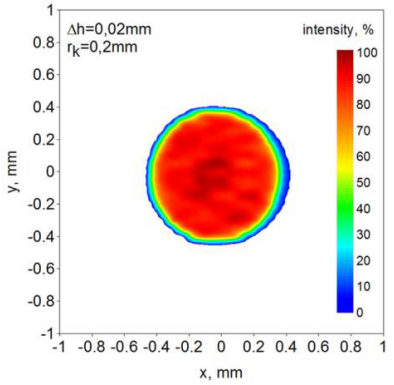

Fig. 3. Percentage distribution of laser beam power. Beam focusing z = 0.

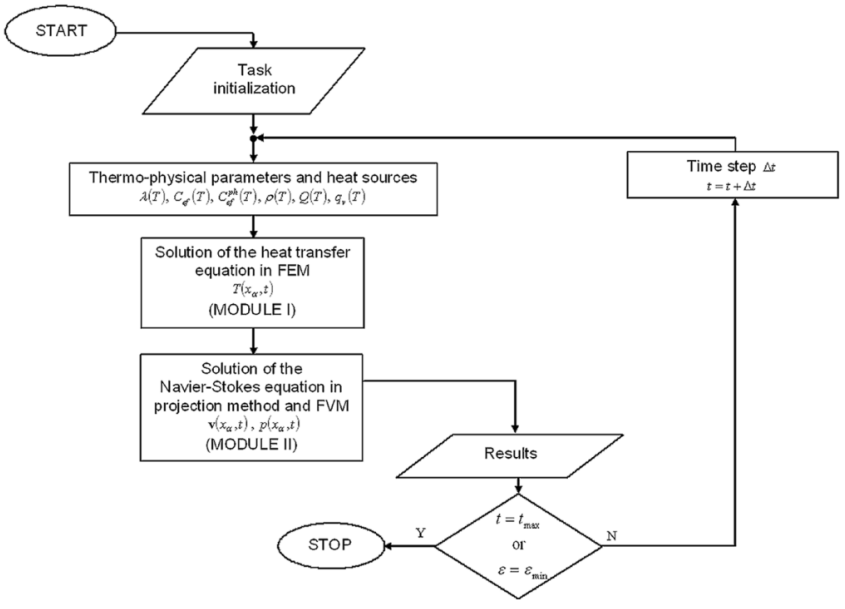

Fig. 4. Solution algorithm.

Differential equations describing thermal phenomena in discussed welding processes are numerically solved using projection method with finite volume method (FVM) [15]. The spatial variables are discretized using staggered grid to avoid odd-even decoupling between the pressure and velocity. Numerical solutions are implemented into the computer solver used for simulation of laser-arc hybrid welding process. The solver is composed of two modules (Fig. 4) for estimating velocity field (module I) in the melted zone determined by solidus temperature (T_s) and temperature field (module II).

3. Results and discussion

The computer simulation of laser-arc hybrid welding process is performed for thin sheets made of S355 steel. The dimensions are 150 mm in length, 30 mm in width, with a thickness of 5 mm. The numerical analysis is made for hybrid welding in geometrical set-up with leading electric arc without a gap. Heat sources parameters are assumed as: laser beam power Q_L = 3000 W, laser beam radius r_0 = 0.45 mm, laser efficiency η_L = 85%, heat source penetration deep s = 7 mm, arc current I = 195 A, welding voltage U = 18.5 V, arc efficiency η_A = 75%. The distance between arc torch and laser beam focal point was set to d = 2 mm and welding speed v =1 m.min^{-1}. In order to verify the correctness of elaborated models, the comparison is made between experimentally determined laser beam profile and interpolated laser beam profile by Kriging algorithm. Fig. 5 shows the comparison of laser power heat source distribution for interpolation grid step Δh = 0.02 mm taking into account experimental data for beam focusing z = 0. The comparison of modelled percentage power intensity distribution with experimentally obtained distribution is illustrated in central axes of the heat source (x = 0 and y = 0).

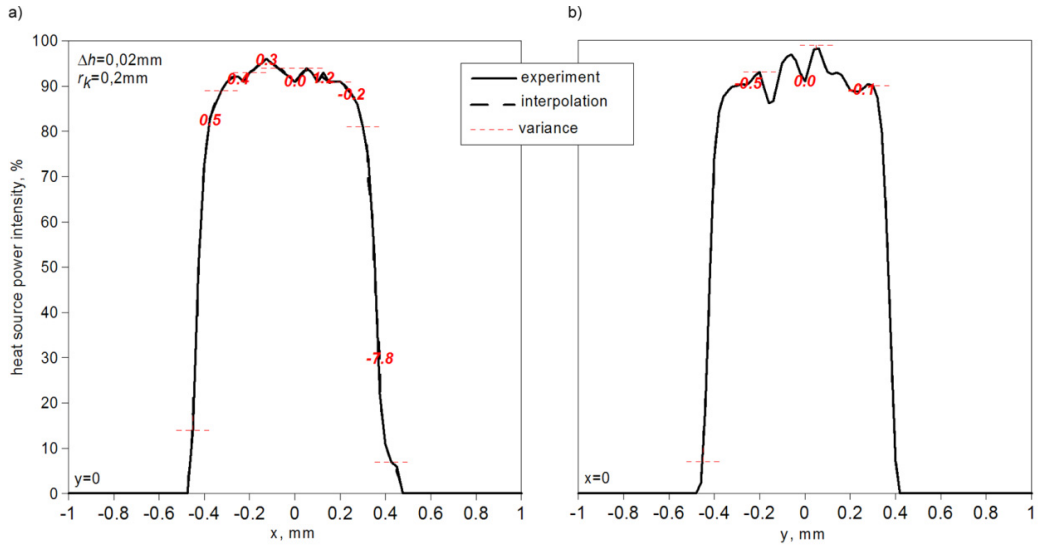

Fig. 5. Comparison of percentage distribution of laser beam power described by interpolation model: a) at central y-axis and b) at central x-axis. Beam focusing z = 0.

Figs. 6–8 show the temperature field and melted material velocity field in hybrid welded joint, where solid line points out melted zone boundary and dashed line marks heat affected zone boundary. Fig. 6 shows temperature distribution at the top surface of the workpiece (z = 0) whereas Fig. 7 illustrates temperature field and melted material velocity field in the longitudinal section, in the middle of heat source activity zone (y = 0). Temperature field and velocity field in the cross section of hybrid laser-arc welded sheets are presented in Fig. 8.

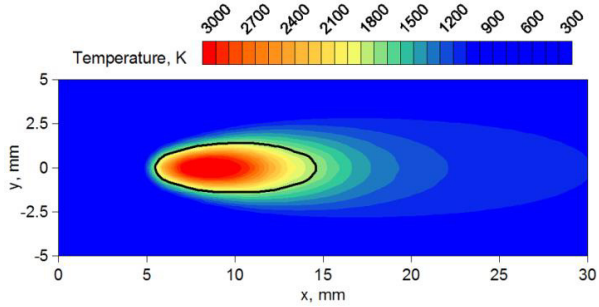

Fig. 6. Calculated temperature field at the top surface ($z = 0$) of the joint.

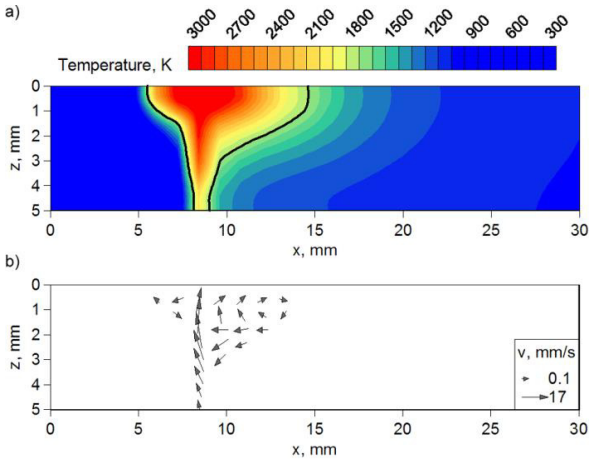

Fig. 7. Calculated: a) temperature field and b) melted material velocity field in the longitudinal section ($y = 0$) of the joint.

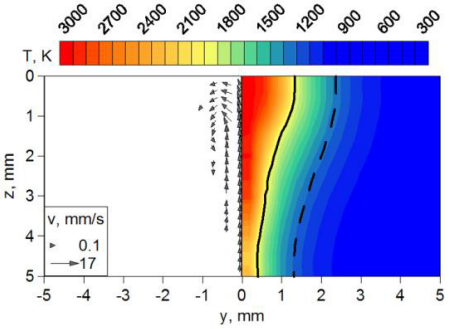

Fig. 8. Calculated: a) temperature field and b) melted material velocity field in the cross section of the joint.

4. Conclusions

In the modelling of hybrid welding process using advanced Yb:YAG laser an appropriate heat source power distribution model is desirable. Application of Kriging method in the numerical analysis allows to specify Yb:YAG laser power distribution in more precise way by reproduction of the real thermal load (Fig. 5) depending on the laser profile obtained for specified industrial laser.

From performed analysis it can be observed that two heat sources in hybrid welding process are cooperating in a single welding pool (Fig. 6 and Fig. 7). The geometry of the weld at the top surface mainly depends on the arc heat source (Fig. 8). Laser beam heat source determines the weld penetration depth, thus at lower parts the weld is more laser-like.

Developed computational model allows assessing the quality of the joint in terms of different process parameters. However, the correctness of developed comprehensive computer tool should be further verified by a large scale experimental research to asses the quality of obtained results.

References

[1] C. Dawes, Laser Welding, Abington Publishing, New York, 1992.
[2] P. Seyffarth, I.V. Krivtsun, Laser-Arc Processes and their Applications in Welding and Material Treatment, Taylor & Francis, USA, 2002.
[3] L. Quintino, R. Miranda, U. Dilthey, D. Iordachescu, M. Banasik, S. Stano, Laser welding of structural aluminium, Advanced Structured Materials 8 (2012) 33–57.

[4] R. Rai, S.M. Kelly, R.P. Martukanitz, T.A. Debroy, Convective heat-transfer model for partial and full penetration keyhole mode laser welding of a structural steel, Metall. Mater. Trans. A 39A (2008) 98–112.
[5] A. Anca, A. Cardona, J. Risso, V.D. Fachinotti, Finite element modeling of welding processes, Appl. Math. Model. 35 (2011) 688–707.
[6] J. Zhou, H.L. Tsai, Modeling of transport phenomena in hybrid laser – MIG keyhole welding, Int. J. Heat Mass Tran. 51 (2008) 4353–4366.
[7] P. Lacki, K. Adamus, Numerical simulation of the electron beam welding process, Comput. Struct. 89 (2011) 977–985.
[8] M. Kubiak, W. Piekarska, Z. Saternus, T. Domański, S. Stano, Simulations and experimental research on laser butt-welded T-joints, Metal 2014: 23rd International Conference on Metallurgy and Materials, 2014, p.726–731.
[9] B.S. Yilbas, Laser heating process and experimental validation, Int. J. Heat Mass Tran. 40 (1997) 1131–1143.
[10] M. Kubiak, W. Piekarska, S. Stano, Modelling of laser beam heat source based on experimental research of Yb:YAG laser power distribution, Int. J. Heat Mass Tran. 83 (2015) 679–689.
[11] O. Wodo, E. Gawrońska, Modeling of two-stage solidification: Part I Model development, Arch. Foundry Eng. 12 (2012) 151–156.
[12] V.B. Biscuola, M.A. Martorano, Micro-macroscopic coupling in the cellular automaton model of solidification, Mater. Res. 13 (2010) 479–484.
[13] J.A. Goldak, Computational Welding Mechanics, Springer NY, USA, 2005.
[14] S. Sakata, F. Ashida, M. Zako, Structural optimization using Kriging approximation, Comp. Meth. Appl. Mech. Eng. 192 (2003) 923–939.
[15] S.V. Patankar, Numerical heat transfer and fluid flow, Taylor & Francis, USA, 1990.